optica

Experimental demonstration of one-shot coherence distillation: realizing *N*-dimensional strictly incoherent operations

SHAO-JIE XIONG,[1,2] ZHE SUN,[1,*] QI-PING SU,[1] ZHENG-JUN XI,[3] LI YU,[1] JIN-SHUANG JIN,[1] JIN-MING LIU,[2] FRANCO NORI,[4,5,7] AND CHUI-PING YANG[1,6,8]

[1]Department of Physics, Hangzhou Normal University, Hangzhou, Zhejiang 310036, China
[2]State Key Laboratory of Precision Spectroscopy, Department of Physics, East China Normal University, Shanghai 200062, China
[3]College of Computer Science, Shaanxi Normal University, Xian 710062, China
[4]Theoretical Quantum Physics Laboratory, RIKEN Cluster for Pioneering Research, Wako-shi, Saitama 351-0198, Japan
[5]Department of Physics, University of Michigan, Ann Arbor, Michigan 48109-1040, USA
[6]Quantum Information Research Center, Shangrao Normal University, Shangrao 334001, China
[7]e-mail: fnori@riken.jp
[8]e-mail: yangcp@hznu.edu.cn
*Corresponding author: sunzhe@hznu.edu.cn

Received 20 April 2021; accepted 10 June 2021 (Doc. ID 427800); published 8 July 2021

We experimentally investigate the one-shot distillation of quantum coherence, which focuses on the transformations from a single copy of a given state into maximally coherent states under various incoherent operations. We present a general proposal to realize a type of strictly incoherent operations (SIOs) that can act on N-dimensional ($N \geq 2$) states. This proposal is suitable for a variety of quantum devices. Based on a linear optical setup, we experimentally demonstrate that the proposed SIO successfully implements pure-to-pure state transformations, and thus the one-shot coherence distillation process is accomplished. The experimental data agree well with the theoretical results and clearly indicate the distillation fidelities, which bound the regions of different coherence distillation rates versus different superposition parameters of input states and different distillation errors.

https://doi.org/10.1364/OPTICA.427800

1. INTRODUCTION

Quantum coherence, exhibiting the fundamental feature of quantum superposition, marks a departure of quantum physics from classical physics. Recently, problems of quantum coherence have attracted considerable attention because these are essential for quantum foundations [1–15] and could also have practical applications in a wide variety of fields, such as quantum cryptography, quantum algorithms, quantum simulations, thermodynamics, quantum metrology, transport theory, and quantum biology [16–27]. To characterize quantum coherence in a mathematically rigorous and physically meaningful framework, the resource theory of quantum coherence was developed [1,28–37]. In this setting, coherence is regarded as a quantum resource that provides a necessary cost in accomplishing useful tasks. For a chosen reference basis $\{|i\rangle\}$, the class of the free states, i.e., the incoherent states, consists of diagonal density matrices in terms of the reference basis, i.e., $\sum_i p_i|i\rangle\langle i| \in \mathcal{I}$. Following this, free operations are incoherent operations (IOs) that act unchangeably on the assemblage of all incoherent states. Many different definitions of IOs are motivated by various physical and mathematical requirements, e.g., maximally IOs (MIOs) [28], IOs [29], dephasing-covariant IOs (DIOs) [30], and strictly IOs (SIOs) [31]. The relations between each of these sets are SIO $\subset$ IO $\subset$ MIO andSIO $\subset$ DIO $\subset$ MIO. There exists a set of incoherent Kraus operators to describe IO, i.e., for $\{K_n\}$ satisfying $\sum_n K_n^\dagger K_n = 1$, every Kraus operator should satisfy $K_n \mathcal{I} K_n^\dagger \subseteq \mathcal{I}$. SIOs are operations for which both $\{K_n\}$ and $\{K_n^\dagger\}$ are sets of incoherent operators.

SIO has a properly strict definition compared to other IOs (e.g., MIO, IO, and DIO), and is easier to theoretically characterize and experimentally implement. Therefore, SIO is widely used in coherence resource theory [9,13,14,32,37]. SIO emerges as a natural set of operations when quantifying the visibility in interferometer experiments [38]. The maximally coherent states can be transformed into any other states using SIO [29]. More importantly, in the one-shot distillation process considered in this paper, even the largest class of free operations, MIO, cannot perform better than SIO [39].

One of the most significant aspects in coherence resource theory is to implement IOs and accomplish state transformations. Much effort has been devoted to the relevant conditions [14,40,41]. Compared to the rapid development of theoretical work, there is a lack of experimental investigation on realizing different classes of IOs. Quite recently, experimental work was reported [42], where a type of SIO in a two-dimensional (2D) space was realized in an optical setup. However, that operation was based on polarization modes and works only in 2D, i.e., it cannot be extended to high-dimensional cases. It is known that it is quite difficult to experimentally realize high-dimensional SIO. One reason is that to manipulate multiple quantum levels collectively is a huge challenge for current technology. To the best of our knowledge, there have been no relevant experimental reports on this. This work fills this gap by *turning the difficult task into a simpler one: repeatedly implementing 2D operations*. Finally, we present a general proposal for the *implementation of a type of N-dimensional SIO and demonstrate it experimentally in a linear optical setup.* The SIO is experimentally realized based on spatial modes, instead of polarization modes, which allows an extension to higher dimensions.

SIOs do not create coherence, but they can distill the coherence if they are provided an input state with coherence. Coherence distillation stands out as one of the most significant ways to practically explore coherence resources [32,43,44], because it extracts the best rate at which one can convert copies of an arbitrary state ρ into copies of pure and maximally coherent states $|\Phi_m\rangle$ (of m-dimension). It is known that $|\Phi_m\rangle$ are important resources and act as the canonical unit resource in various quantum tasks. Coherence distillation reveals the operational meaning in coherence resource theory and introduces a basic coherence measure, i.e., distillable coherence.

Note that the standard distillation proposal is at the asymptotic limit [32], i.e., assuming an unbounded number of copies of the system considered. In a realistic setting, only a finite supply of states is available. Moreover, it is a huge challenge to collectively manipulate coherent states over a large number of systems. Therefore, it is necessary to consider a more general scenario to distill maximally coherent states from a finite number of state copies [39,45–47]. In particular, [39] introduced a one-shot coherence distillation that requires a single copy of a given state and adopts an ε-error fidelity to extract the distillation rate, matching the realistic restrictions on state transformations. This scenario facilitates precise characterization of the experimentally feasible rates of coherence distillation. There are several possible applications of one-shot coherence distillation. It can be treated as quantum extraction of the intrinsic randomness of measurements [15]. Another promising application is to prepare coherence resources for direct use in quantum key distribution and quantum algorithms [16–18]. To our knowledge, our work is the first to *experimentally demonstrate one-shot coherence distillation in a realistic setting.* From our results, one can find *how to prepare coherent states, select the target states, and transform the state via the proposed SIO.*

2. ONE-SHOT COHERENCE DISTILLATION

In asymptotic coherence distillation [32], an unbounded number of state copies is needed, which is, however, quite difficult to achieve in a realistic setting. To overcome this difficulty, [39] introduced one-shot coherence distillation tolerating an error ε, which is measured by

$$C^{(1),\varepsilon}_{d,\mathcal{O}}(\rho) := \log \max\{m \in \mathbb{N} | F_{\mathcal{O}}(\rho, |\Phi_m\rangle) \geq 1-\varepsilon\}, \qquad (1)$$

where the superscript "(1)" indicates that only a single copy of the given state ρ (or pure state $|\psi\rangle$) and the m-dimensional maximally coherent state $|\Phi_m\rangle \equiv \sum_{i=1}^{m} |i\rangle/\sqrt{m}$ are included. The asymptotic version is obtained in the limit $C^{\infty,\varepsilon}_{d,\mathcal{O}}(\rho) = \lim_{\varepsilon\to 0}\lim_{n\to\infty} C^{(1),\varepsilon}_{d,\mathcal{O}}(\rho^{\otimes n})/n$. The definition of the distillation fidelity $F_{\mathcal{O}}(\rho, |\Phi_m\rangle)$ is

$$F_{\mathcal{O}}(\rho, |\Phi_m\rangle) = \max_{\Lambda\in\mathcal{O}} \langle \Lambda(\rho), |\Phi_m\rangle\rangle, \qquad (2)$$

where $\mathcal{O}$ denotes a class of IOs, and $\langle A, B\rangle = \mathrm{Tr}(A^\dagger B)$ is the Hilbert–Schmidt inner product. This distillation fidelity describes the maximal conversion rate from a given state to the maximally coherent state $|\Phi_m\rangle$ by optimizing the IOs. The value of $F_{\mathcal{O}}(\rho, |\Phi_m\rangle)$ depends on the chosen dimension m of $|\Phi_m\rangle$ and the type of IOs. The error ε in Eq. (1) has various meanings. Note that the definition of the concept of one-shot coherence distillation in Eq. (1) is based on the concept of distillation fidelity, i.e., $F_{\mathcal{O}}(\rho, |\Phi_m\rangle)$, which characterizes the distinguishability between the output state of the SIO and the perfect resource state. The error ε provides a finite tolerance of distinguishability.

The key step in one-shot coherence distillation is to realize proper IOs. In this work, only pure-to-pure state transformations are studied because: (i) pure states are important resources in quantum tasks and (ii) theoretical results are clear for pure states, e.g., the one-shot distillable coherence of pure states under MIO, DIO, IO, or SIO is exactly the same [39].

A. Proposal for SIO

Figure 1 shows a general proposal to realize SIO in N-dimensional cases, where we divide the operations into several steps. The transformation from the input state $|\psi\rangle$ to the target state $|\phi\rangle$ can be realized by n ($n \leq N-1$) steps. At each step, an IO (in fact, SIO here) works on two components of the given state $|\psi\rangle$, and the corresponding superposition parameters are changed as needed (details in Supplement 1). Since the elementary operation belongs to SIO, the following multi-step operations also belong to SIO [40]. The reason that we choose accumulated 2D operations to achieve N-dimensional operations is that manipulating two quantum levels is much more stable and efficient than manipulating multiple levels collectively using current technology. In Fig. 1, we illustrate the experimental implementation of each step. In realistic settings, IOs in a primary system are usually performed by introducing ancillary systems. In module **S**, two components $|i\rangle$ and $|j\rangle$ of the primary system should be coupled to the ancillary qubit $|\tilde{q}\rangle_0$ ($q = 0, 1$), which can be used repeatedly. Some designed operations can be performed on the two-qubit space (details in Supplement 1). Focusing on the primary modes, 2D SIOs are realized. Module **RS** has two functions: (i) reset the ancillary modes $|\tilde{q}\rangle_0$ to the initial situations by employing another ancillary qubit $|\tilde{q}\rangle_k$ ($q = 0$, 1 and $k \neq 0$) and (ii) repeat the operations of module **S** working on a pair of primary components different from that in the previous step. At the nth step, there are 2^{n-1} copies of the target state corresponding to 2^{n-1} groups of ancillary modes. In addition, $a_{n,1}, a_{n,2}, \ldots$, and $a_{n,2^{n-1}}$ satisfy $\sum_k^{2^{n-1}} a^2_{nk} = 1$. One can obtain the target state deterministically by performing tomography on all the outputs, but probabilistically by reading part of the outputs. Such a simple combination of two types of modules (modules **S** and **RS**) provides a significant advantage of our proposal. This can be conveniently applied in a variety of quantum controllable systems, where the correlations and manipulations between two-level systems can be performed stably and efficiently. In the following sections, we experimentally realize SIO in an optical setup.

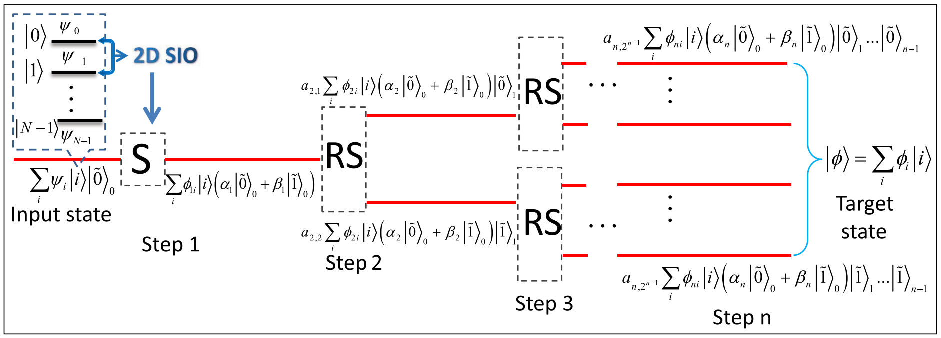

Fig. 1. Proposal for realizing the SIO in N-dimensional cases by multiple steps. It implements pure-to-pure state transformations, i.e., $|\psi\rangle = \sum_{i=0}^{N-1} \psi_i |i\rangle \to |\phi\rangle = \sum_{i=0}^{N'-1} \phi_i |i\rangle$, with the dimensionality $N' \le N$. At each step, only two components are manipulated (see the inset). Two types of modules are needed in the experimental implementation. In module **S**, an ancillary qubit $|\tilde{q}\rangle_0$ should be coupled to two components (e.g., $|i\rangle$ and $|j\rangle$) of the primary system, and the two-dimensional SIO is realized in this module. Module **RS** has two functions: (i) reset the ancillary modes $|\tilde{q}\rangle_0$ to the initial situation; (ii) repeat the operations of module **S** working on two primary components different from those in the previous step. At the nth step, the superposition coefficients ϕ_{ni} carry the superposition information of the target state ϕ_i.

B. SIO in Optics

Let us start with 2D SIO in optics. We employ the spatial modes of the photons, $|0\rangle$ and $|1\rangle$, to describe the primary system state, which makes possible the extension to high dimensions and has essential differences in the basic design and motivation from previous studies [42]. The polarization modes $|V\rangle$ and $|H\rangle$ (i.e., vertical and horizontal modes) act as the ancillary qubit. The experimental setup is shown in the **S** module in optics in Fig. 2. Here, we change $|i\rangle$ and $|j\rangle$ to $|0\rangle$ and $|1\rangle$ for simplicity. The input state of the total system is $|\psi\rangle|V\rangle = (\alpha|0\rangle + \beta|1\rangle)|V\rangle$ with real numbers α and β. The angles θ_1 and θ_2 of the half-wave plates (HWPs) $P_{1,2}^{ij}$ are adjusted as needed. Then, the map $\Lambda(|\psi\rangle\langle\psi|) = K_1|\psi\rangle\langle\psi|K_1^\dagger + K_2|\psi\rangle\langle\psi|K_2^\dagger$ can be achieved with the Kraus operators

$$K_1 = \cos 2\theta_1 |0\rangle\langle 0| + \sin 2\theta_2 |1\rangle\langle 1|,$$

$$K_2 = \cos 2\theta_2 |0\rangle\langle 1| + \sin 2\theta_1 |1\rangle\langle 0|. \tag{3}$$

When the parameters satisfy $|\alpha|^2 \sin(4\theta_1) = |\beta|^2 \sin(4\theta_2)$, one can obtain the pure output state, i.e., $\Lambda(|\psi\rangle\langle\psi|) = |\phi\rangle\langle\phi|$.

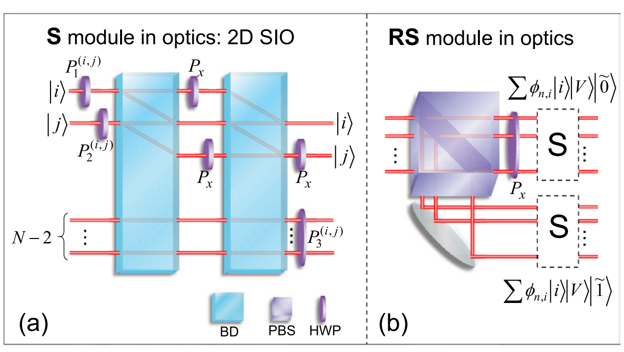

Fig. 2. **S** and module **RS** in optical setups. The devices are half-wave plates (HWP), beam displacers (BD), and polarizing beam splitters (PBS). The angles of the HWP $P_1^{i,j}$ and $P_2^{i,j}$ are adjusted as needed. All the angles of the HWP P_x are set to $\pi/4$, which performs the inversions $|H\rangle \to |V\rangle$ and $|V\rangle \to |H\rangle$. The angle of $P_3^{i,j}$ is adjusted according to the outputs of the i, j paths. In the **RS** module in optics, a PBS is employed to reset the ancillary polarization modes to the initial situations. $|\tilde{0}\rangle$ and $|\tilde{1}\rangle$ label the new ancillary qubits encoded into the split path groups.

According to the definition of SIO [14,40], the operations described by the Kraus operators in Eq. (3) belong to SIO. For more applications, if the operations at the output (**S** module in Fig. 2) are changed, ensuring that the superposition state of polarization modes in one path are orthogonal to that of another path, other kinds of IOs will be realized (details in Supplement 1).

To realize the **RS** module, a polarization beam splitter (PBS) is employed to introduce a new pair of spatial modes, i.e., $|\tilde{0}\rangle_k$ and $|\tilde{1}\rangle_k (k \neq 0)$, coupled to the polarization modes. Along each mode $|\tilde{q}\rangle_k$, the polarization modes are reset into the initial situation of $|V\rangle$. Then, module **S** is applied again.

3. EXPERIMENTAL DEMONSTRATION OF ONE-SHOT COHERENCE DISTILLATION

A single-photon source is produced by pumping a type I β-barium borate crystal with ultraviolet pulses at a 405 nm centered wavelength. One photon is directly detected as a trigger. The other one is prepared in a pure state of the spatial modes $|i\rangle$ $(i = 0, 1, 2, \ldots)$.

A. Example 1: Three-Dimensional Distillation

The input state is chosen as

$$|\psi^3\rangle = \sqrt{\alpha}|2\rangle + \sqrt{(1-\alpha)/2}(|0\rangle + |1\rangle), \tag{4}$$

where $\alpha \in [0, 1]$. Superscript "3" denotes the dimensionality. Based on the distillation fidelity in Eq. (2), one should obtain the target states closest to the maximally coherent states by performing proper IOs. In the region $\alpha \in [0, 1/2]$, the distillation fidelity $F_{\mathcal{O}}(|\psi^3\rangle, |\Phi_2\rangle)$ is proved to be 1 (details in Supplement 1). Theoretically, $|\psi^3\rangle$ can be perfectly converted to the maximally coherent state $|\Phi_2\rangle = (|0\rangle + |1\rangle)/\sqrt{2}$.

Figure 3 shows an experimental setup to accomplish the transformation from $|\psi^3\rangle$ to $|\Phi_2\rangle$. It is a simplified two-step version of the general proposal in Fig. 1. After the PBS, only one beam displacer (BD) is needed to combine two paths into one, achieving dimension reduction. The initial state $|\psi^3\rangle$ can be prepared based on the spatial modes. Parameters $\theta_{1,2,3,4,5}$, depending on coefficient α (details in Supplement 1), can be adjusted as needed. One obtains $|\Phi_2\rangle$ by doing spatial tomography at the output [measurement setup shown in Supplement 1, Fig. S1(b)]. The

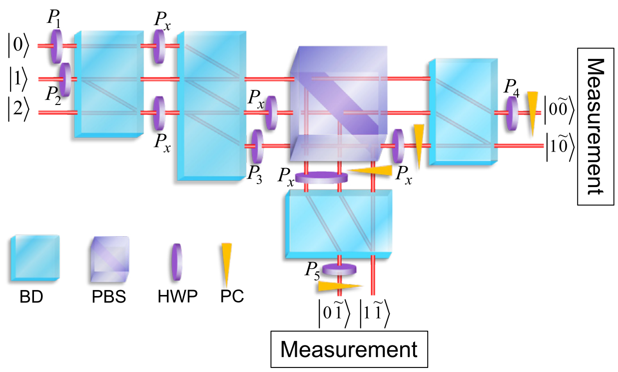

Fig. 3. Experimental implementation of the one-shot distillation processes for the 3D input state, i.e., an optical setup for the SIO converting a 3D pure state into a 2D pure state. The angles of the HWPs $P_{1,2,3,4,5}$ are adjusted as needed. All the angles of P_x are set to $\pi/4$. The devices are quarter-wave plates (QWP), phase compensators (PC), and interference filters (IF).

photons are detected by single-photon detectors equipped with 10 nm interference filters. The extinction rate of our interferometer can reach over 500:1, and the average fidelity between the ideal states and actual states can reach higher than 99%. In fact, the proposal in Fig. 3 provides a general SIO that can convert 3D pure states to 2D pure states obeying the majorization condition (details in Supplement 1).

In the region $\alpha \in (1/2, 1]$, the distillation fidelity becomes $F_{\mathcal{O}}(|\psi^3\rangle, |\Phi_2\rangle) = \frac{1}{2}(\sqrt{\alpha} + \sqrt{1-\alpha})^2$, which implies that the maximally coherent state $|\Phi_2\rangle$ cannot be reached. Instead, a possible target state becomes $|\phi_{3\to 2}\rangle = \sqrt{\alpha}|0\rangle + \sqrt{1-\alpha}|1\rangle$. The device to realize the transformation $|\psi^3\rangle \to |\phi_{3\to 2}\rangle$ is shown in Supplement 1.

In Fig. 4(a), experimental data agree well with the theoretical results and show the errors of the distillation fidelities $F_{\mathcal{O}}(|\psi^3\rangle, |\Phi_3\rangle)$ (denoted by triangles) and $F_{\mathcal{O}}(|\psi^3\rangle, |\Phi_2\rangle)$ (denoted by rhombuses) versus the superposition coefficient α. The distillation error $\varepsilon \equiv 1 - F_{\mathcal{O}}$. The 3D maximally coherent state is defined as $|\Phi_3\rangle = (|0\rangle + |1\rangle + |2\rangle)/\sqrt{3}$. The data show that in the region $\alpha \in [0, 1/2]$, $F_{\mathcal{O}}(|\psi^3\rangle, |\Phi_2\rangle)$ approaches one, while in the region $\alpha \in [1/2, 1]$, $F_{\mathcal{O}}(|\psi^3\rangle, |\Phi_2\rangle)$ decreases to 1/2 for increasing values of α.

According to the definition in Eq. (1), in Fig. 4(a), the regions of different distillation rates are bounded by the fidelities $F_{\mathcal{O}}(|\psi^3\rangle, |\Phi_2\rangle)$ and $F_{\mathcal{O}}(|\psi^3\rangle, |\Phi_3\rangle)$. If a zero error $\varepsilon = 0$ is strictly required, the distillable coherence will be measured as $C_{d,\mathcal{O}}^{(1),\varepsilon=0}(|\psi^3\rangle) = \log 2$ in the region $\alpha \in [0, 1/2]$, except at the point $\alpha = 1/3$, where $C_{d,\mathcal{O}}^{(1),\varepsilon=0}(|\psi^3\rangle) = \log 3$. However, when $\alpha > 1/2$, the distillation fidelity cannot reach one any more, which implies that the ideal coherence resource cannot be distilled from state $|\psi^3\rangle$. However, in practical tasks, a finite tolerance $\varepsilon \neq 0$ is usually accepted. For example, if an accepted error is $\varepsilon = 0.1$, the distillable coherence will be $C_{d,\mathcal{O}}^{(1),\varepsilon=0.1}(|\psi^3\rangle) = \log 3$ in a larger region about $\alpha \in [0.0838, 0.6495]$, and $C_{d,\mathcal{O}}^{(1),\varepsilon=0.1}(|\psi^3\rangle) = \log 2$ in $\alpha \in [0, 0.0838) \cup (0.6495, 0.8]$. Such an example clearly shows the fact that when a larger error is tolerated, (i.e., the requirement for similarity between the input state and the target state is reduced as a trade-off), a higher distillation rate will be obtained.

B. Example 2: Four-Dimensional Distillation

We choose a 4D input state (for $\alpha \in [0, 1/2]$):

$$|\psi^4\rangle = \sqrt{\alpha}(|0\rangle + |1\rangle) + \sqrt{1/2 - \alpha}(|2\rangle + |3\rangle). \tag{5}$$

For the 2D maximally coherent state $|\Phi_2\rangle$, the distillation fidelity $F_{\mathcal{O}}(|\psi^4\rangle, |\Phi_2\rangle)$ is proven to be one over the entire range of $\alpha \in [0, 1/2]$. Thus, a reasonable target state is $|\Phi_2\rangle = (|2\rangle + |3\rangle)/\sqrt{2}$. The device to realize the transformation from $|\psi^4\rangle \to |\Phi_2\rangle$ is shown in Supplement 1.

For the 3D maximally coherent state $|\Phi_3\rangle$, the distillation fidelity is $F_{\mathcal{O}}(|\psi^4\rangle, |\Phi_3\rangle) = \frac{2}{3}(\sqrt{\alpha} + \sqrt{1-2\alpha})^2$ in the region $\alpha \in [0, 1/6] \cup [1/3, 1/2]$. Therefore, a reasonable target state is $|\phi_{4\to 3}\rangle = \sqrt{2\alpha}|1\rangle + \sqrt{(1/2-\alpha)}(|2\rangle + |3\rangle)$, while in the region $\alpha \in [1/6, 1/3]$, the fidelity is $F_{\mathcal{O}}(|\psi^4\rangle, |\Phi_3\rangle) = 1$. Thus, the maximally coherent state $|\Phi_3\rangle$ is the target.

The transformation $|\psi^4\rangle \to |\phi_{4\to 3}\rangle$ can be easily accomplished (details in Supplement 1). However, to realize $|\psi^4\rangle \to |\Phi_3\rangle$ is much more complicated. It can be achieved by either the general method (in Fig. 1) with three steps or the simplified proposal in Fig. 3 with the extension to a four-path input and two more module **S**'s at the outputs.

In Fig. 4(b), we show the experimental data of the errors of the distillation fidelity $F_{\mathcal{O}}(|\psi^4\rangle, |\Phi_2\rangle)$ (denoted by rhombuses) and $F_{\mathcal{O}}(|\psi^4\rangle, |\Phi_3\rangle)$ (denoted by triangles) versus the superposition

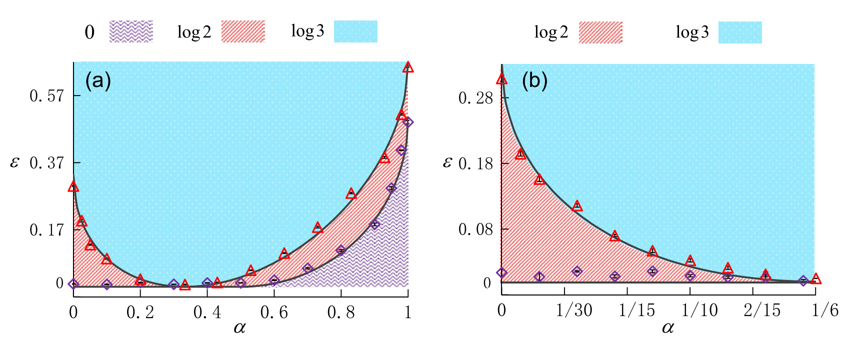

Fig. 4. Experimental data of the errors ε of the distillation fidelity versus the superposition coefficient α. The regions of different colors and fill patterns correspond to different distillation rates defined in Eq. (1), with the values in the annotations (0, log 2, log 3) at the top of the figure. (a) Case of the 3D input state $|\psi^3\rangle$ given in Eq. (4). The experimental data of the distillation fidelity $F_{\mathcal{O}}(|\psi^3\rangle, |\Phi_3\rangle)$ are denoted by triangles, and the experimental data of $F_{\mathcal{O}}(|\psi^3\rangle, |\Phi_2\rangle)$ are denoted by rhombuses. Solid lines correspond to theoretical results. (b) Cases of the 4D input state $|\psi^4\rangle$ given in Eq. (5). The experimental data of $F_{\mathcal{O}}(|\psi^4\rangle, |\Phi_3\rangle)$ are denoted by triangles, and the experimental data of $F_{\mathcal{O}}(|\psi^4\rangle, |\Phi_2\rangle)$ are denoted by rhombuses. $|\Phi_2\rangle$ and $|\Phi_3\rangle$ are the maximally coherent states of 2D and 3D, respectively.

coefficient α. In experiments, we test only the region $\alpha \in [0, 1/6]$, where one can see that if the zero error is strictly defined, the distillable coherence is measured by $C_d^{(1),\varepsilon=0}(|\psi^4\rangle) = \log 2$, except at the point of $\alpha = 1/6$, where $C_d^{(1),\varepsilon=0}(|\psi^4\rangle) = \log 3$. If a finite error $\varepsilon \neq 0$ is allowed, one will obtain a higher rate $C_d^{(1),\varepsilon}(|\psi^4\rangle) = \log 3$ in a wider region of α conditioned by $F_{\mathcal{O}}(|\psi^4\rangle, |\Phi_3\rangle) \geq (1 - \varepsilon)$.

4. CONCLUSION

We have studied the problems of implementing IOs in a realistic optical system and demonstrated the one-shot coherence distillation process experimentally. A general proposal was introduced to realize an important SIO applicable to high dimensions. Two sets of states were chosen as input states, and their distillation fidelities were obtained analytically. We clearly demonstrate the process of one-shot coherence distillation, i.e., the preparation of the resource states, selection of the target states, and the state transformation under the proposed SIO. Experimental data agree well with the theoretical results and reveal the relation between coherence distillation rates and finite tolerance errors for different given states. For extensions, additional unitary operations can be added at the outputs to realize other kinds of IOs, i.e., some transformations of pure-to-mixed state and mixed-to-mixed state can also be realized.

The experimental proposal of N-dimensional SIO is suitable for other quantum systems. For example, in superconducting circuit-QED systems [48, 49], one can employ a superconducting qudit [50–52] with N levels to be the primary system and another superconducting qubit as the ancillary system. By alternately performing the coupling between the primary and ancillary systems and the resonant pulses between the levels involved, one can realize SIO.

Funding. National Key Research and Development Program of China (2016YFA0301802); National Natural Science Foundation of China (11174081, 11375003, 11774076, 11775065, 11974096, 61472114, 61671280, 91950112); Natural Science Foundation of Zhejiang Province (LY17A050003); Natural Science Foundation of Shanghai (16ZR1448300); Army Research Office (W911NF-18-1-0358); Foundational Questions Institute Fund (FQXi-IAF19-06); Japan Society for the Promotion of Science (JP20H00134, JPJSBP120194828); Japan Science and Technology Agency (JPMJCR1676).

Disclosures. The authors declare no conflicts of interest.

Data availability. Data underlying the results presented in this paper are not publicly available at this time but may be obtained from the authors upon reasonable request.

Supplemental document. See Supplement 1 for supporting content.

REFERENCES

1. A. Streltsov, G. Adesso, and M. B. Plenio, "Quantum coherence as a resource," Rev. Mod. Phys. **89**, 041003 (2017).
2. M. L. Hu, X. Y. Hu, J. C. Wang, Y. Peng, Y. R. Zhang, and H. Fan, "Quantum coherence and geometric quantum discord," Phys. Rep. **762**, 1–100 (2018).
3. A. Streltsov, U. Singh, H. S. Dhar, M. N. Bera, and G. Adesso, "Measuring quantum coherence with entanglement," Phys. Rev. Lett. **115**, 020403 (2015).
4. M. Lostaglio, K. Korzekwa, D. Jennings, and T. Rudolph, "Quantum coherence, time-translation symmetry, and thermodynamics," Phys. Rev. X **5**, 021001 (2015).
5. T. R. Bromley, M. Cianciaruso, and G. Adesso, "Frozen quantum coherence," Phys. Rev. Lett. **114**, 210401 (2015).
6. C. Napoli, T. R. Bromley, M. Cianciaruso, M. Piani, N. Johnston, and G. Adesso, "Robustness of coherence: an operational and observable measure of quantum coherence," Phys. Rev. Lett. **116**, 150502 (2016).
7. Y. Yao, X. Xiao, L. Ge, and C. P. Sun, "Quantum coherence in multipartite systems," Phys. Rev. A **92**, 022112 (2015).
8. M. Ringbauer, T. R. Bromley, M. Cianciaruso, L. Lami, W. Y. Sarah Lau, G. Adesso, A. G. White, A. Fedrizzi, and M. Piani, "Certification and quantification of multilevel quantum coherence," Phys. Rev. X **8**, 041007 (2018).
9. L. Lami, B. Regula, and G. Adesso, "Generic bound coherence under strictly incoherent operations," Phys. Rev. Lett. **122**, 150402 (2019).
10. X. Wang, A. Miranowicz, Y. X. Liu, C. P. Sun, and F. Nori, "Sudden vanishing of spin squeezing under decoherence," Phys. Rev. A **81**, 022106 (2010).
11. W. Zhong, Z. Sun, J. Ma, X. Wang, and F. Nori, "Fisher information under decoherence in Bloch representation," Phys. Rev. A **87**, 022337 (2013).
12. W. Nie, Z. H. Peng, F. Nori, and Y. X. Liu, "Topologically protected quantum coherence in a superatom," Phys. Rev. Lett. **124**, 023603 (2020).
13. B. Yadin, J. Ma, D. Girolami, M. Gu, and V. Vedral, "Quantum processes which do not use coherence," Phys. Rev. X **6**, 041028 (2016).
14. E. Chitambar and G. Gour, "Comparison of incoherent operations and measures of coherence," Phys. Rev. A **94**, 052336 (2016).
15. X. Yuan, H. Zhou, Z. Cao, and X. Ma, "Intrinsic randomness as a measure of quantum coherence," Phys. Rev. A **92**, 022124 (2015).
16. T. Sashki, Y. Yamamoto, and M. Koashi, "Practical quantum key distribution protocol without monitoring signal disturbance," Nature **509**, 475–478 (2014).
17. M. Hillery, "Coherence as a resource in decision problems: the Deutsch-Jozsa algorithm and a variation," Phys. Rev. A **93**, 012111 (2016).
18. H. L. Shi, S. Y. Liu, X. H. Wang, W. L. Yang, Z. Y. Yang, and H. Fan, "Coherence depletion in the Grover quantum search algorithm," Phys. Rev. A **95**, 032307 (2017).
19. I. Buluta and F. Nori, "Quantum simulators," Science **326**, 108–111 (2009).
20. I. M. Georgescu, S. Ashhab, and F. Nori, "Quantum simulation," Rev. Mod. Phys. **86**, 153 (2014).
21. K. D. Wu, Z. B. Hou, G. Y. Xiang, C. F. Li, G. C. Guo, D. Y. Dong, and F. Nori, "Detecting non-Markovianity via quantified coherence: theory and experiments," npj Quantum Inf. **6**, 55 (2020).
22. M. Lostaglio, D. Jennings, and T. Rudolph, "Description of quantum coherence in thermodynamic processes requires constraints beyond free energy," Nat. Commun. **6**, 6383 (2015).
23. R. Demkowicz-Dobrzanski and L. Maccone, "Using entanglement against noise in quantum metrology," Phys. Rev. Lett. **113**, 250801 (2014).
24. G. Kiesslich, E. Scholl, T. Brandes, F. Hohls, and R. J. Haug, "Noise enhancement due to quantum coherence in coupled quantum dots," Phys. Rev. Lett. **99**, 206602 (2007).
25. E. Romero, R. Augulis, V. Novoderezhkin, M. Ferretti, J. Thieme, D. Zigmantas, and R. van Grondelle, "Quantum coherence in photosynthesis for efficient solar-energy conversion," Nat. Phys. **10**, 676 (2014).
26. N. Lambert, Y. N. Chen, Y. C. Chen, C. M. Li, G. Y. Chen, and F. Nori, "Quantum biology," Nat. Phys. **9**, 10 (2013).
27. C. M. Li, N. Lambert, Y. N. Chen, G. Y. Chen, and F. Nori, "Witnessing quantum coherence: from solid-state to biological systems," Sci. Rep. **2**, 885 (2012).
28. J. Aberg, "Quantifying superposition," arXiv:quant-ph/0612146 (2006).
29. T. Baumgratz, M. Cramer, and M. B. Plenio, "Quantifying coherence," Phys. Rev. Lett. **113**, 140401 (2014).
30. E. Chitambar and G. Gour, "Critical examination of incoherent operations and a physically consistent resource theory of quantum coherence," Phys. Rev. Lett. **117**, 030401 (2016).
31. F. G. S. L. Brandão and G. Gour, "Reversible framework for quantum resource theories," Phys. Rev. Lett. **115**, 070503 (2015).
32. A. Winter and D. Yang, "Operational resource theory of coherence," Phys. Rev. Lett. **116**, 120404 (2016).
33. F. Levi and F. Mintert, "A quantitative theory of coherent delocalization," New J. Phys. **16**, 033007 (2014).
34. Z. W. Liu, K. F. Bu, and R. Takagi, "One-shot operational quantum resource theory," Phys. Rev. Lett. **123**, 020401 (2019).
35. C. L. Liu and D. L. Zhou, "Deterministic coherence distillation," Phys. Rev. Lett. **123**, 070402 (2019).

36. E. Chitambar and G. Gour, "Quantum resource theories," Rev. Mod. Phys. **91**, 025001 (2019).
37. A. Streltsov, S. Rana, P. Boes, and J. Eisert, "Structure of the resource theory of quantum coherence," Phys. Rev. Lett. **119**, 140402 (2017).
38. T. Biswas, M. G. Díaz, and A. Winter, "Interferometric visibility and coherence," Proc. R. Soc. A **473**, 20170170 (2017).
39. B. Regula, K. Fang, X. Wang, and G. Adesso, "One-shot coherence distillation," Phys. Rev. Lett. **121**, 010401 (2018).
40. S. P. Du, Z. F. Bai, and Y. Guo, "Conditions for coherence transformations under incoherent operations," Phys. Rev. A **91**, 052120 (2017).
41. Z. J. Xi, Y. Luo, and L. H. Shao, "Coherence manipulation under non-cohering operations," J. Phys. A **52**, 375301 (2019).
42. K. D. Wu, T. Theurer, G. Y. Xiang, C. F. Li, G. C. Guo, M. B. Plenio, and A. Streltsov, "Quantum coherence and state conversion: theory and experiment," npj Quantum Inf. **6**, 22 (2020).
43. E. Chitambar, A. Streltsov, S. Rana, M. N. Bera, G. Adesso, and M. Lewenstein, "Assisted distillation of quantum coherence," Phys. Rev. Lett. **116**, 070402 (2016).
44. K. D. Wu, Z. B. Hou, H. S. Zhong, Y. Yuan, G. Y. Xiang, C. F. Li, and G. C. Guo, "Experimentally obtaining maximal coherence via assisted distillation process," Optica **4**, 454–459 (2017).
45. K. Fang, X. Wang, L. Lami, B. Regula, and G. Adesso, "Probabilistic distillation of quantum coherence," Phys. Rev. Lett. **121**, 070404 (2018).
46. Q. Zhao, Y. C. Liu, X. Yuan, E. Chitambar, and A. Winter, "One-shot coherence distillation: towards completing the picture," IEEE Trans. Inform. Theory **65**, 6441–6453 (2019).
47. K. F. Bu, U. Singh, S. M. Fei, A. K. Pati, and J. D. Wu, "Maximum relative entropy of coherence: an operational coherence measure," Phys. Rev. Lett. **119**, 150405 (2017).
48. X. Gu, A. F. Kockum, A. Miranowicz, Y. X. Liu, and F. Nori, "Microwave photonics with superconducting quantum circuits," Phys. Rep. **718-719**, 1–102 (2017).
49. A. F. Kockum and F. Nori, "Quantum bits with Josephson Junctions," in *Fundamentals and Frontiers of the Josephson Effect*, (F. Tafuri, ed.), (Vol. **286**, Springer Series in Materials Science), (Springer, 2019), Chapter 17, pp. 703–741.
50. M. Neeley, M. Ansmann, R. C. Bialczak, M. Hofheinz, E. Lucero, A. D. O'Connell, D. Sank, H. Wang, J. Wenner, A. N. Cleland, M. R. Geller, and J. M. Martinis, "Emulation of a quantum spin with a superconducting phase qudit," Science **325**, 722–725 (2009).
51. Y. Han, X. Q. Luo, T. F. Li, W. Zhang, S. P. Wang, J. S. Tsai, F. Nori, and J. Q. You, "Time-domain grating with a periodically driven qutrit," Phys. Rev. Appl. **11**, 014053 (2019).
52. A. Miranowicz, S. K. Ozdemir, J. Bajer, G. Yusa, N. Imoto, Y. Hirayama, and F. Nori, "Quantum state tomography of large nuclear spins in a semiconductor quantum well: optimal robustness against errors as quantified by condition numbers," Phys. Rev. B **92**, 075312 (2015).